Supplement of Biogeosciences, 17, 215–230, 2020
https://doi.org/10.5194/bg-17-215-2020-supplement

Biogeosciences Open Access EGU

Supplement of

Bacterial degradation activity in the eastern tropical South Pacific oxygen minimum zone

Marie Maßmig et al.

Correspondence to: Anja Engel (aengel@geomar.de)

This supplementary includes the following supporting information:

Supplementary Methods: Detailed description of dissolved organic carbon and dissolved oxygen flux calculations.

Supplementary Discussion: Discussion about the incubation of extracellular enzyme samples under N_2 atmosphere.

Supplementary Figure 1: Oxygen content, temperature and chlorophyll concentrations of the remaining transects not represented as figure within the manuscript.

Supplementary Figure 2: Total verses cell-specific bacterial production rates that were sampled at *in situ* oxygen concentrations < 20 µmol O_2 kg^{-1}.

Supplementary Figure 3: Original measurements before temperature correction of extracellular enzyme rates at different *in situ* oxygen concentrations.

Supplementary Figure 4: Original measurements before temperature correction of extracellular enzyme rates with all samples incubated under N_2 atmosphere irrespective of the *in situ* oxygen concentration.

Supplementary Table 1: Cruise, date, positions, sampled depths and bottom depth of all stations represented within the manuscript.

Supplementary Table 2: Average and standard deviation at different oxygen regimes of all discussed parameters.

Supplementary Methods:

Diapycnal fluxes of oxygen and dissolved organic carbon

The mixing of DOC and oxygen across density surfaces is derived following Fischer et al. (2013) and Schafstall et al. (2010). Gradients of DOC where calculated between sampled bottles assuming a constant gradient in between while oxygen gradients were derived by fitting a linear trend over 3 m intervals, as oxygen is available on a much higher vertical resolution of 1dbar.

The diapycnal flux of solutes, i.e. DOC and oxygen, is calculated as

$$\Phi_S = -K_\rho \nabla C_S$$

Where $\nabla C_S$is the vertical gradient of the solute – in case of oxygen the concretion is converted from µmol kg^{-1} to µmol m^{-3} beforehand – and K_ρ is the diapycnal diffusivity of mass. We assume K_ρ to be equal to the diffusivity of DOC and oxygen, i.e. $K_\rho = K_{DOC} = K_{DO}$ as done by Fischer et al. (2013) for oxygen.

The diapycnal diffusivity is calculated following Osborn (1980):

$$K_\rho = \Gamma \frac{\varepsilon}{N^2}$$

Where $\Gamma = 0.2$ is the mixing efficiency, ε (m^2 s^{-3}) is the dissipation rate of turbulent kinetic energy calculated by integrating the shear spectra derived from measurements on a freefalling microstructure probe at stations G-N & Q-T (Sea & Sun Technology, MSS90D, S/N26 up to CTD 43, S/N 73 afterwards) (Schafstall et al., 2010), and N (s^{-1}) is the buoyancy frequency derived from CTD downcast profiles over 7 dbar intervals where DOC and oxygen were measured as well.

To calculate K_ρ, data from CTD profiles were combined with nearby microstructure profiles conducted directly before or after the CTD profile which existed for 12 profiles. For each solute gradient between two samples a $K_\rho$value was derived from dissipation and buoyancy frequency averaged between the potential densities of the two solutes samples. The mean K_ρ profile exhibits only weak vertical variations (Figure 5a) therefore a constant $K_\rho = 10^{-3} m^2 s^{-1}$ was used to calculate fluxes.

For each profile a Φ_S profile is calculated in 20 m depth bins, from these a mean profile of diapycnal flux is derived. Subsequent, the vertical divergence of the mean flux profile of DOC or oxygen is given by $\nabla\Phi_S = -\frac{\partial}{\partial z}\Phi_S$.

The error estimates of these terms are calculated following Schafstall et al. (2010), with the error of the mean $K_\rho$given by:

$$\Delta K_\rho = K_\rho \left[\left(\frac{\Delta\Gamma}{\Gamma}\right)^2 + \left(\frac{\Delta\varepsilon}{\varepsilon}\right)^2 + \left(\frac{\Delta N^2}{N^2}\right) \right]^{\frac{1}{2}}$$

And the error of the mean flux by

$$\Delta\Phi_S = \Phi_S \left[\left(\frac{\Delta\Gamma}{\Gamma}\right)^2 + \left(\frac{\Delta\varepsilon}{\varepsilon}\right)^2 + \left(\frac{\Delta N^2}{N^2}\right) + \left(\frac{\Delta\nabla C_S}{\nabla C_S}\right) \right]^{\frac{1}{2}}$$

Where K_ρ and Φ_S are the mean profiles calculated from the individual profiles in 20 m depth bins, a constant $\Delta\Gamma = 0.04$ is used (Schafstall et al., 2010), the error of dissipation $\Delta\varepsilon$is the 95%-confidence interval derived by bootstrapping, $\Delta N^2$and $\Delta\nabla C_S$are the standard deviations of the mean. Bootstrapping and standard deviations are performed on the values of the individual profiles in 20 m bins. The error of the change in the diapycnal flux over depth is derived by error propagation from the flux.

Supplementary Discussion:

Incubation of extracellular enzyme samples under N_2 atmosphere

Enzyme rates of suboxic waters have been obtained by incubating samples under N_2 atmosphere to reduce oxygen concentrations. For the assessment of extracellular enzyme rates we chose to incubate samples at oxic and reduced oxygen concentrations depending on oxygen concentrations at *in situ* depth (see methods for details). Incubation conditions slightly influenced the resulting enzyme rates. Incubating samples from depths with *in situ* oxygen concentrations <5 µmol kg^{-1} under N_2 atmosphere, instead of under atmospheric oxygen concentrations, yielded on average 2-27% higher rates. Consequently, the differences in rates between oxic and suboxic waters became reduced, when all samples were incubated under N_2 atmosphere (supplementary Fig. 3 and 4). However, the observed trends over depth remained similar. Possible reasons for higher extracellular enzyme rates after incubation under N_2 atmosphere are changes in (i) pH, (ii) the abundance of oxygen radicals and/or (iii) changes in enzyme production. (i) Higher extracellular enzyme rates after incubations at low oxygen concentrations are less likely driven by the resulting increase in pH (Δ 0.4), since earlier studies rather suggested that extracellular enzyme rates decrease with pH (Endres et al., 2014; Piontek et al., 2013). (ii) Oxygen radicals can destroy enzymes (Elstner, 1990). Since our incubations were not completely anoxic, an influence of oxygen radicals on enzyme activity cannot be excluded, but would appear under aerobic and N_2 atmosphere. (iii) Finally, an enhanced production of enzymes within the 12 hours of incubation time might be the reason for higher rates after incubations under N_2 atmosphere. It has been shown before that enzymes can be produced within minutes (Both et al., 1972), making this explanation likely. The final reason for higher enzyme productions under N_2 atmosphere remains a matter of speculation, but supports the trends seen in the depth profiles and does not restrict the interpretation of the extracellular enzyme data.

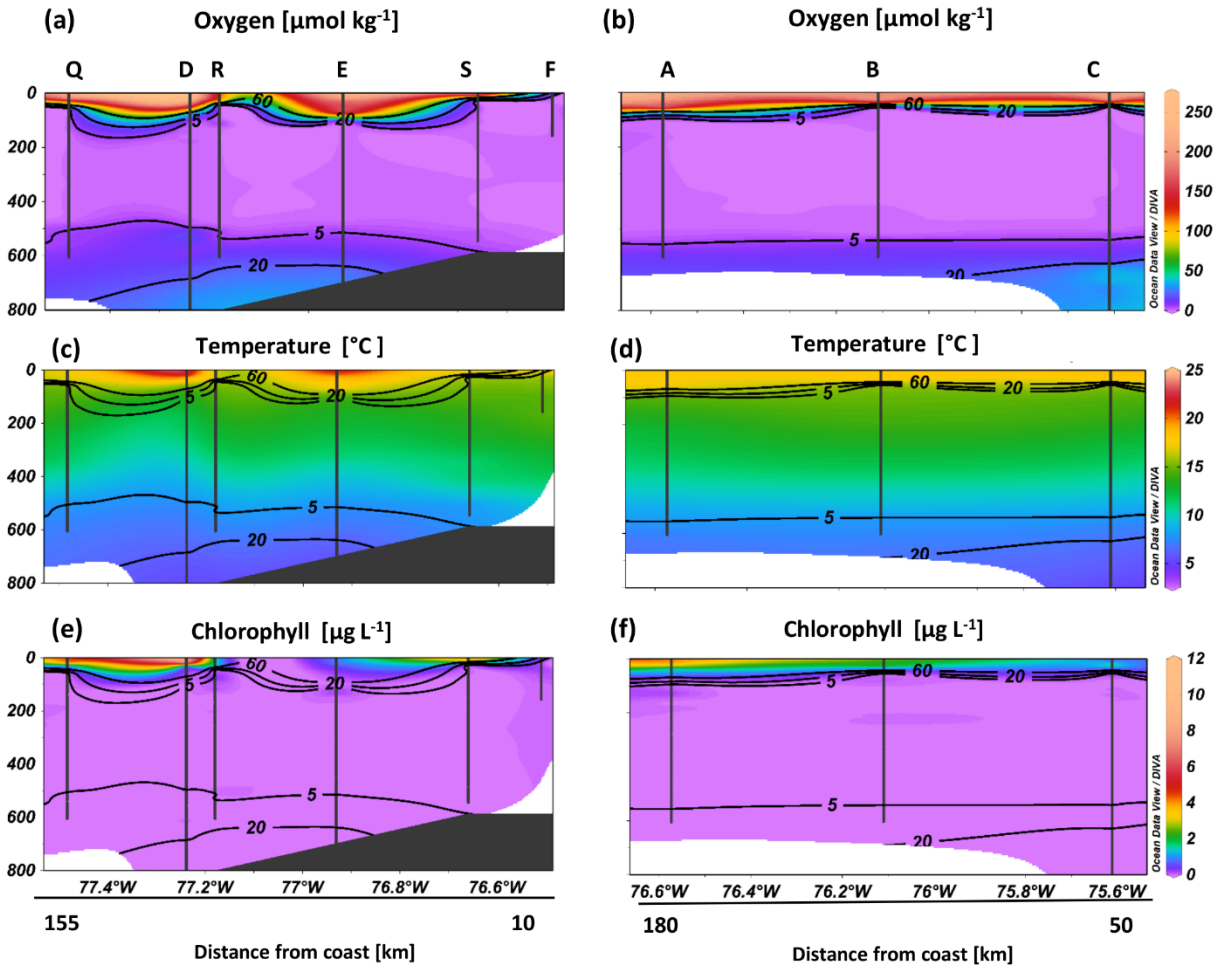

Supplementary Figure 1: Oxygen content (a, b), temperature (c, d) and chlorophyll concentrations (e-f) of the remaining two transects that are not represented in Figure 3 in the manuscript.

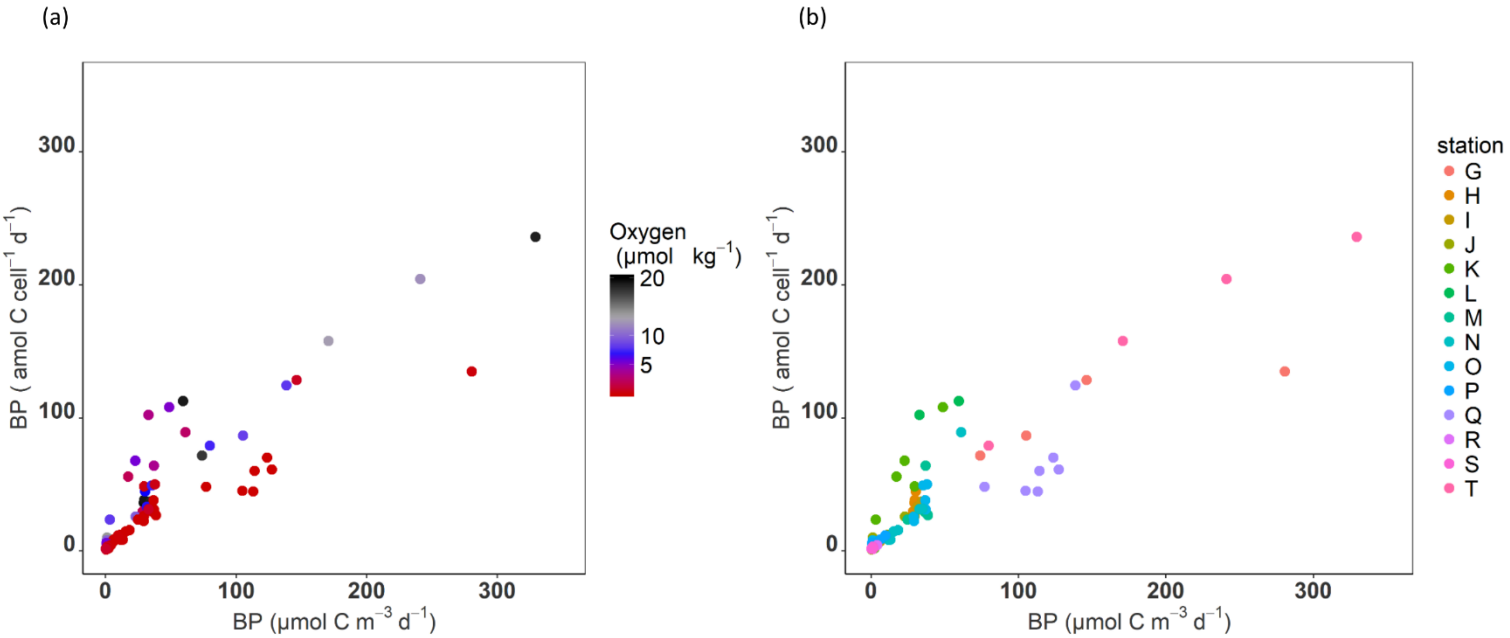

Supplementary Figure 2: Total verses cell-specific bacterial production that were at *in situ* oxygen concentrations < 20 µmol O_2 kg^{-1} with oxygen concentrations (a) and stations (b) indicated by color-coding.

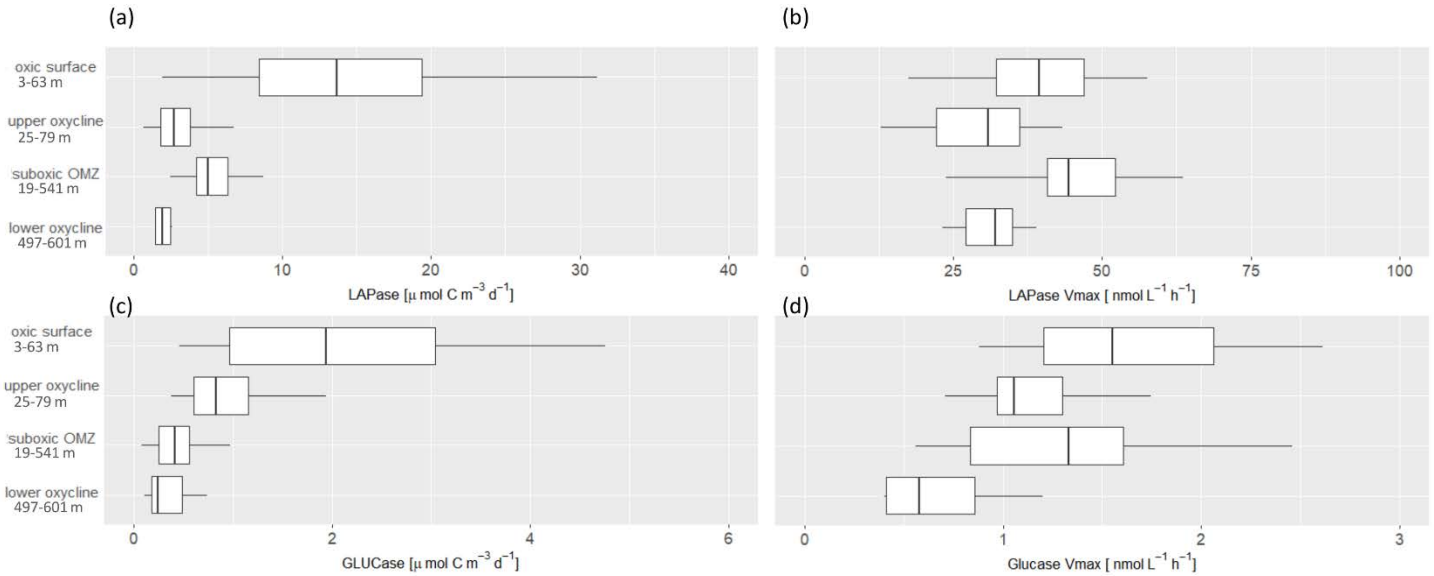

Supplementary Figure 3: Original measurements before temperature correction of extracellular enzyme rates at different *in situ* oxygen concentrations for comparison with measured enzyme rates that were all incubated under N_2 atmosphere (supplementary Figure 4). Degradation rates of dissolved amino acids (DHAA) by leucine-aminopeptidase (LAPase) **(a)**, total potential LAPase rates (V_{max}) **(b)**, degradation rates of high molecular weight dissolved carbohydrates (DCHO) by ß-glucosidase (GLUCase) **(c)** and Glucase V_{max} **(d)** at different oxygen regimes.

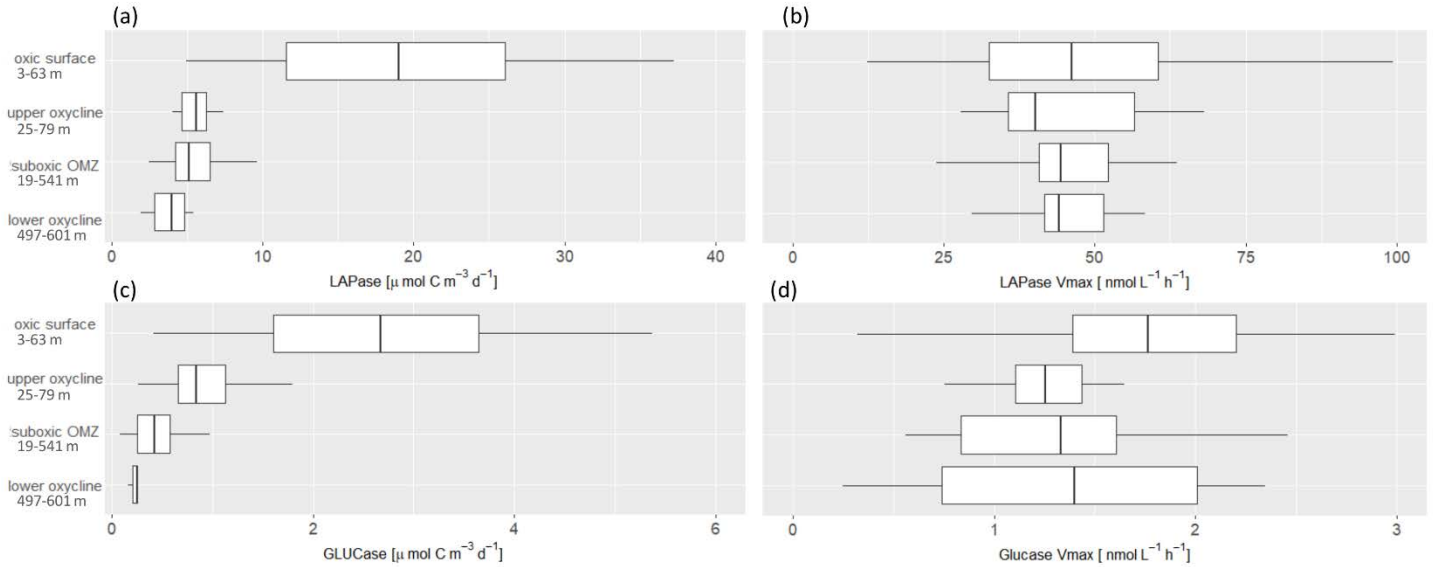

Supplementary Figure 4: Original measurements before temperature correction of extracellular enzyme rates with all samples incubated under N_2 atmosphere irrespective of the *in situ* oxygen concentration. Degradation rates of dissolved amino acids (DHAA) by leucine-aminopeptidase (LAPase) **(a)** total potential LAPase rates (V_{max}) **(b)**, degradation rates of high molecular weight dissolved carbohydrates (DCHO) by ß-glucosidase (GLUCase) **(c)** Glucase V_{max} **(d)** at different oxygen regimes.

Supplentary Table 1: Cruise, date, positions, sampled depths and bottom depth of all stations represented within the manuscript. Extracellular enzyme rates were sampled at stations A-K, whereas some depths were not used for further analyses, since the standard deviation was over 30%. Bacterial biomass production was sampled at stations G-T. Stations G-T were included in the estimation of carbon and oxygen loss rates. Cell abundance was sampled at every station.

Cruise	Station	Latitude	Longitude	Date	Sampled Depth						Bottom Depth
M138	A	-15.5393	-75.6149	06/19/2017	3	17	24	28	39		2507
					99	197	396	596	1499		
M138	B	-15.8595	-76.1099	06/21/2017	5	18	40	50	53		2624
					90	199	398	600			
M138	C	-16.1593	-76.5711	06/21/2017	3	13	19	58	63		3679
					79	99	149	197	347	600	
M138	D	-13.9971	-76.6598	06/16/2017	3	8	19	48	70		586
					98	117	197	397	498	541	
M138	E	-14.2988	-77.1796	06/17/2017	19	38	47	66	97		4702
					147	198	299	398	497	601	
M138	F	-14.7596	-77.4829	06/23/2017	9	28	48	53	99		4154
					148	197	297	397	497	601	
M136	G	-12.2248	-77.1795	04/27/2017	4	20	25	30	39		75
					49	59	72				
M136	H	-12.3584	-77.3621	04/25/2017	3	6	27	39	48		194
					58	68	79	98	128		
M136	I	-12.453	-77.4918	04/26/2017	4	18	28	39	49		403
					59	73	199				
M136	J	-12.5807	-77.6731	04/29/2017	4	28	49	68	78		973
					99	195	393	448	498	598	
M136	K	-12.338	-78.0512	04/26/2017	9	50	75	99	148		1970
					157	199	299	398	499	599	
M136	L	-12.2782	-77.2493	04/20/2017	4	9	13	19	23		130
					28	43	48	58			
M136	M	-12.3882	-77.40297	04/19/2017	3	19	39	55	65		242
					90	98	199	238			
M136	N	-12.4134	-77.4425	04/21/2017	3	18	50	99	124		307
					149	174	224	272	300		
M136	O	-12.5226	-77.5834	04/20/2017	4	29	39	49	59		751
					79	89	98	147	597	745	
M136	P	-12.9873	-78.2471	04/21/2017	4	29	49	60	74		5410
					99	196	296	396	599	800	
M136	Q	-13.8938	-76.5101	04.12.2017	4	10	15	19	30		166
					39	50	69	99	128	159	
M136	R	-14.1878	-76.9312	04/13/2017	5	14	29	49	81		3042
					101	123	199	399	599		
M136	S	-14.3986	-77.2389	04/14/2017	1	49	89	99	148		5149
					198	299	399	499	599		
M136	T	-12.2254	-77.1797	04/24/2017	4	19	24	28	49		76

Supplementary Table 2: Average and standard deviation at different oxygen regimes of all discussed parameters as total rates and cell abundance **(a)** and cell-specific rates **(b)**. Rates are indicated as temperature corrected *in situ* rates and original measurements during incubation. Differences between oxygen regimes were tested with a *Wilcoxon test* (W) and correlation with the *Spearman Rank correlation* (S).

a				original measurements		temperature corrected				
parameter	**station**	**oxygen regime**	**n**	**mean**	**SD**	**mean**	**SD**	**oxygen regime**	**test statistics**	***p*-value**
bacterial production [µmol C m^{-3} d^{-1}]	G-T	top oxic	34	194	189	603	618	top oxic-OMZ	W=145	<0.001
		top high hypoxic	11	58	61	126	140	OMZ, low hypoxic (correlation BP vs. O_2)	S=51692, rho=0.1	0.4
		top low hypoxic	17	43	38	87	87			
		OMZ	48	26	32	37	53			
		bottom low hypoxic	5	5	3	1	1	OMZ-bottom low hypoxic	W=30	<0.01
		oxyclines	33	42	47	87	108			
	H-S	OMZ	46	22	24	30	35	oxycline-OMZ	W=439	0.1
		oxyclines	25	27	30	50	66			
	G&T	OMZ	2	120	57	213	95	oxycline-OMZ	W=9	0.89
		oxyclines	8	91	57	204	132			
degradation rates of DHAA by LAPase [µmol C m^3 d^{-1}]	A-K	top oxic	20	13.9	7.6	16.3	9.2	oxycline-OMZ	W=701	<0.001
		top high hypoxic	6	4.5	3.0	4.9	3.3			
		top low hypoxic	9	2.4	1.2	2.6	1.3			
		OMZ	40	5.5	2.1	5.5	2.1			
		bottom low hypoxic	6	2.4	1.6	2.0	1.3			
		oxyclines	21	3.0	2.1	3.1	2.3			
degradation rates of DCHO by GLUCase [µmol C m^3 d^{-1}]	A-K	top oxic	22	2.74	2.45	3.5	3.3	oxycline-OMZ	W=184	<0.01
		top high hypoxic	7	1.45	1.02	1.7	1.2			
		top low hypoxic	8	0.76	0.51	0.9	0.6			
		OMZ	38	0.69	1.29	0.7	1.3			
		bottom low hypoxic	3	0.36	0.33	0.3	0.2			
		oxyclines	18	1.00	0.80	1.1	1.0			
LAPase Vmax [nmol L h^{-1}]	A-K	top oxic	22	39.2	13.3	45.2	15.7	oxycline-OMZ	W=1012	<0.001
		top high hypoxic	10	41.1	24.0	45.5	26.4			
		top low hypoxic	10	28.9	13.6	31.5	14.9			
		OMZ	49	49.9	22.1	49.5	20.8			
		bottom low hypoxic	6	31.3	6.0	26.0	5.0			
		oxyclines	26	34.1	17.7	35.6	20.1			
GLUCase Vmax [nmol L h^{-1}]	A-K	top oxic	26	1.6	0.6	2.1	0.7	oxycline-OMZ	W=555.5	0.4
		top high hypoxic	9	1.4	0.5	1.7	0.5			
		top low hypoxic	11	1.0	0.3	1.1	0.4			
		OMZ	41	1.6	1.6	1.6	1.5			
		bottom low hypoxic	4	0.7	0.4	0.5	0.3			
		oxyclines	24	1.1	0.5	1.2	0.6			
cell abundance [x10^5 cells mL^{-1}]	A-T	top oxic	52	19.2	9.2			oxycline-OMZ	3031	<0.01
		top high hypoxic	16	9.4	3.0					
		top low hypoxic	20	8.4	3.0					
		OMZ	93	9.0	5.0					
		bottom low hypoxic	14	1.2	0.1					
		oxyclines	51	6.6	4.3					

100

b				original measurements		temperature corrected				
parameter	**station**	**oxygen regime**	**n**	**mean**	**SD**	**mean**	**SD**	**oxygen regime**	**test statistics**	***p*-value**
cell-specific bacterial production [amol C cell d^{-1}]	G-T	top oxic	34	92	78	282	265	OMZ, low hypoxic (correlation BP vs. O_2)	S=36615, rho=0.36	<0.01
		top high hypoxic	11	50	36	105	85			
		top low hypoxic	17	46	27	89	62			
		OMZ	48	22	19	31	33			
		bottom low hypoxic	5	35	23	11	7			
		oxyclines	33	45	29	82	72			
	H-S	OMZ	46	20	16	26	25	oxycline-OMZ	W=301	<0.001
		oxyclines	25	37	23	58	51			
	G&T	OMZ	2	73	5	132	4	oxycline-OMZ	W=6	0.7
		oxyclines	8	71	34	158	78			
cell-specific Degradation rates of DHAA by LAPase [amol C $cell^{-1}$ d^{-1}]	A-K	top oxic	20	6.5	3.4	7.6	4.2	bottom low hypoxic - remaining regimes	W=380	<0.01
		top high hypoxic	6	4.6	3.1	5.0	3.4			
		top low hypoxic	9	3.1	1.6	3.3	1.7			
		OMZ	40	12.3	14.4	11.7	12.2			
		bottom low hypoxic	6	21.5	15.4	17.9	12.7			
		oxyclines	21	8.8	11.5	8.0	9.3			
cell-specific Degradation rates of DCHO by GLUCase [amol C $cell^{-1}$ d^{-1}]	A-K	top oxic	22	1.3	1.2	1.7	1.5	bottom low hypoxic - remaining regimes	W=150	0.33
		top high hypoxic	7	1.4	1.1	1.6	1.3			
		top low hypoxic	8	1.1	0.8	1.2	0.9			
		OMZ	38	1.2	1.7	1.1	1.6			
		bottom low hypoxic	3	3.2	3.2	2.3	2.3			
		oxyclines	18	1.6	1.6	1.6	1.3			
cell-specific LAPase Vmax [amol cell h^{-1}]	A-K	top oxic	22	23.1	15.1	26.4	16.9	bottom low hypoxic - remaining regimes	W=523	<0.001
		top high hypoxic	10	44.0	29.7	48.8	32.6			
		top low hypoxic	10	40.0	22.8	43.4	24.7			
		OMZ	49	103.5	114.2	99.0	97.4			
		bottom low hypoxic	6	274.0	51.6	227.3	42.6			
		oxyclines	26	95.5	104.7	87.9	83.88			
cells-specific GLUCase Vmax [amol cell h^{-1}]	A-K	top oxic	26	0.9	0.4	1.1	0.4	bottom low hypoxic - remaining regimes	W=314	<0.01
		top high hypoxic	9	1.5	0.6	1.6	0.7			
		top low hypoxic	11	1.3	0.5	1.5	0.5			
		OMZ	41	2.7	2.4	2.7	2.3			
		bottom low hypoxic	4	6.0	3.6	5.0	2.8			
		oxyclines	24	2.1	2.2	2.1	1.7			

References_supplement

Both, G. W., McInnes, J. L., Hanlon, J. E., May, B. K. and Elliott, W. H.: Evidence for an accumulation of messenger RNA specific for extracellular protease and its relevance to the mechanism of enzyme secretion in bacteria, J. Mol. Biol., 67(2), 199–217, doi:10.1016/0022-2836(72)90236-7, 1972.

Elstner, E. F., Ed.: Der Sauerstoff: Biochemie, Biologie, Medizin, BI-Wiss_Verl, Mannheim., 1990.

Endres, S., Galgani, L., Riebesell, U., Schulz, K.-G. and Engel, A.: Stimulated Bacterial Growth under Elevated pCO2: Results from an Off-Shore Mesocosm Study, edited by S. Dupont, PLoS One, 9(6), e99228, doi:10.1371/journal.pone.0099228, 2014.

Fischer, T., Banyte, D., Brandt, P., Dengler, M., Krahmann, G., Tanhua, T. and Visbeck, M.: Diapycnal oxygen supply to the tropical North Atlantic oxygen minimum zone, Biogeosciences, 10(7), 5079–5093, doi:10.5194/bg-10-5079-2013, 2013.

Osborn, T. R.: Estimates of the local rate of vertical diffusion from dissipation measurements, J. Phys. Oceanogr., 10(1), 83–89, doi:10.1175/1520-0485, 1980.

Piontek, J., Borchard, C., Sperling, M., Schulz, K. G., Riebesell, U. and Engel, A.: Response of bacterioplankton activity in an Arctic fjord system to elevated pCO_2: results from a mesocosm perturbation study, Biogeosciences, 10(1), 297–314, doi:10.5194/bg-10-297-2013, 2013.

Schafstall, J., Dengler, M., Brandt, P. and Bange, H.: Tidal-induced mixing and diapycnal nutrient fluxes in the Mauritanian upwelling region, J. Geophys. Res., 115(C10), C10014, doi:10.1029/2009JC005940, 2010.